

Tracing the evolution of eccentric precessing binary black holes: a hybrid approach

Amitesh Singh ^{1,*} Nathan K. Johnson-McDaniel ^{1,†} Anuradha Gupta ^{1,‡} and Khun Sang Phukon ^{2,§}

¹*Department of Physics and Astronomy, The University of Mississippi, University, Mississippi 38677, USA*

²*School of Physics and Astronomy and Institute for Gravitational Wave Astronomy,
University of Birmingham, Edgbaston, Birmingham, B15 2TT, United Kingdom*

(Dated: June 13, 2025)

To describe a general bound binary black hole system, we need to consider orbital eccentricity and the misalignment of black holes' spin vectors with respect to the orbital angular momentum. While binary black holes produced through many formation channels have negligible eccentricity close to merger, they often have a non-negligible eccentricity at formation, and dynamical interactions could produce binaries with non-negligible eccentricity in the bands of current and proposed gravitational-wave (GW) detectors. Another quantity that carries information about the formation channel is the angle between each black hole's spin vector and the binary's orbital angular momentum (referred to as the spin tilt) at formation. The spin tilts inferred in GW astronomy are usually those when the binary is in the band of a GW detector, but these can differ significantly from those at formation. Therefore, it is necessary to evolve the binary back in time to compute the tilts at formation. For many formation scenarios, the tilts in the formal limit of infinite orbital angular momentum, also known as tilts at infinity, are a good approximation to those at formation. We thus generalize the publicly available `tilts_at_infinity` code to compute the tilts at infinity for eccentric, spin-precessing binaries. This code employs hybrid post-Newtonian evolution, starting with orbit-averaged evolution for higher frequencies and then transitioning to precession-averaged evolution to compute the tilts at infinity. We find that the transition frequency used in the quasicircular case still gives acceptably small errors in the eccentric case, and show that eccentricity and hybrid evolution both have a significant effect on the tilts at infinity for many binaries. Finally, we give examples of cases where the tilts at infinity are and are not a good approximation to the tilts at formation in the eccentric case.

I. INTRODUCTION

Binary black hole (BBH) detection is now a fairly frequent occurrence, thanks to the recent improvements in detector sensitivity and other advancements in hardware and software for the current ground-based LIGO and Virgo detectors [1, 2]. The LIGO-Virgo-KAGRA Collaboration (LVK) has detected more than 90 compact binary coalescences so far [3], including BBHs, binary neutron stars, and black hole-neutron star binaries. This number is expected to increase rapidly as the current detectors (including KAGRA [4]) continue to increase their sensitivity [5] and next generation detectors come online, both ground-based detectors like Einstein Telescope [6] and Cosmic Explorer [7] as well as space-based detectors like LISA [8].

Understanding the mechanisms that form the observed BBHs is a major goal of gravitational-wave (GW) astronomy, and the distributions of the binaries' inferred parameters (e.g., masses, spin vectors, eccentricities, and luminosity distances) provide important clues about these mechanisms [9, 10]. In particular, the distribution of spin tilts is crucial to distinguishing between different BBH formation channels. An isotropic distribution of black hole spins is indicative of dynamical formation, while aligned spins suggest an isolated formation process (see [11]). In addition to spin tilts, orbital eccentricity plays an important role in distinguishing binary formation

channels. Over long timescales, GWs efficiently reduce orbital eccentricity by extracting angular momentum from the system [12]. Consequently, binaries formed through isolated channels are typically expected to circularize before entering the detection band of current ground-based GW detectors. Conversely, some binaries originating from dynamical channels, such as active galactic nuclei or globular clusters, are anticipated to retain non-negligible eccentricities at detection frequencies [13]. Over the last few years, there have been claims that some of the observed BBHs could be eccentric [13–18]. With the advent of upcoming detectors like LISA and next-generation GW detectors, the prospects of detecting eccentric BBHs will only keep increasing. Ref. [19] shows that if one neglects a small but non-zero residual eccentricity at 10 Hz ($e_{10\text{ Hz}} \leq 0.05$), it can lead to significant biases in the spin tilts when evolving the binary backwards to a large separation ($\sim 10^4$ times the binary's total mass in geometrized units) to find the spin tilts at a point closer to the binary's formation. Hence, we need to be prepared for a possible observation of a precessing binary with non-negligible eccentricity and need to be able to compute the tilts at infinity in such cases.

The measurements of spin tilts in the third observing run were not very precise, with no significant difference between the posterior distributions of spin tilts at infinity and at the reference frequency for either the individual events [20] or for the population [21]. However, their precision will improve with the sensitivity of the detectors, e.g., in the plus-era of detectors [22, 23]. In particular, [23] showed that it is possible to measure the tilts at detection frequency with an accuracy of 0.06 rad (with 90% credible interval) for certain comparable-mass quasicircular binaries with the plus-era sensitivity of the LIGO and Virgo detectors (expected to be attained during the

* amiteshsingh487@gmail.com

† nkjm.physics@gmail.com

‡ agupta1@olemiss.edu

§ k.s.phukon@bham.ac.uk

fifth observing run [5]). Thus, for the third-generation detectors like Cosmic Explorer and the Einstein Telescope, which are ~ 10 times more sensitive than the plus-era detectors, it may be possible to measure these tilts with an accuracy of ~ 0.006 rad for certain binaries. (Ref. [24] finds an accuracy of 0.02 rad for Cosmic Explorer alone for one case, though with different parameters, notably a somewhat smaller total mass and spins, than the binary considered in [23] that gives the best accuracy.) Ref. [25] predicts that LISA will be able to measure these tilts with a 90% credible interval of width 0.003 rad in some cases.

The tilts inferred in the detectors' sensitive band can be significantly different from those at formation, as is illustrated in, e.g., [23]. Ref. [20] showed that spin tilts at infinity are a good approximation to those at formation for many formation scenarios. The spin tilts at infinity are obtained in the limit where the binary's orbital angular momentum $L \rightarrow \infty$, since in this limit the amplitude of spin precession goes to zero. This limit is attained theoretically for exactly quasicircular binaries, though in practice there is always a finite uncertainty in the tilts at formation from two-spin precession (proportional to $1/L$), even though in principle (albeit not in practice) this uncertainty can be arbitrarily small. However, for eccentric binaries, the limit of infinite orbital separation corresponds to the limit where the eccentricity $e \nearrow 1$, and the orbital angular momentum approaches a finite value, as can be seen from the expressions in [12], as discussed in Refs. [20, 26]. Nevertheless, we still compute the tilts at infinity for eccentric binaries: The precession-averaged evolution [20] we use to perform this computation is insensitive to the presence of eccentricity, and the tilts at infinity still provide a well-defined (idealized) reference point for these cases. Moreover, in some eccentric formation scenarios, L at formation will still be large enough that the uncertainties in the tilts will be small. However, dynamically formed binaries with extremely high eccentricities at formation ($e \simeq 0.99999999$, or one minus eccentricity of $\sim 10^{-8}$), which lead to a significant eccentricity in the band of ground-based detectors, can possess much lower angular momentum values, as low as $L/M^2 \simeq 0.1$ (using the population synthesis data from [27]). In those cases, one will not want to compute the tilts at infinity as an approximation to the tilts at formation, but may rather be able to compute the tilts at formation to a good approximation by evolving backwards to a finite (and not particularly large) separation, as we will show with an example.

There exist codes to evolve quasicircular, precessing BBHs to infinite separation [20, 28]. However, there are not yet any public codes for evolving eccentric, precessing binaries to infinity. It is important to have such a code, particularly to ensure that the systematic errors in the computation of spin tilts at infinity remain smaller than the anticipated statistical uncertainties for future GW observations. Thus, we extend the `tilts_at_infinity` code [20] in the LALSuite GW data analysis package [29] to evolve eccentric, precessing BBHs in a hybrid approach: we use orbit-averaged post-Newtonian (PN) evolution code [30] (hereafter referred to as the orbit-averaged code) at small orbital separations and switch to faster but less accurate precession-averaged equations [20] at large

orbital separations, where the precession-averaged evolution is sufficiently accurate. This hybrid approach provides a more accurate way to compute the tilts at infinity than just using precession-averaged evolution as in [26]. While we wait for this code to be reviewed by the LVK collaboration to be officially included in LALSuite master [29], an unreviewed version of the code is publicly available at [31] via a fork of LALSuite.

We find that using the same transition orbital velocity (depending only on the binary's mass ratio) as that obtained in the quasicircular case in [20] gives acceptably small errors in the tilts at infinity due to the choice of the transition orbital velocity. Here the errors are computed using the difference in the spin tilts at infinity obtained using the empirically determined transition orbital velocity as in [20], and half of that value. These errors are all lower than 10^{-2} in the cosines of the tilts at infinity and thus smaller than the anticipated statistical errors for observations in the upcoming fifth observing run of the advanced GW detector network [23]. We do not demand the same accuracy of 10^{-3} that is achieved for the quasicircular code [20], since the eccentric orbit-averaged evolution is less accurate than the quasicircular one. In particular, the eccentric orbit-averaged evolution only includes the leading spin-orbit and spin-spin terms (i.e., 2PN accuracy), while, [20] finds that in the quasicircular case the first PN correction to the spin-orbit terms (at 2.5PN) leads to differences as large as ~ 0.1 .¹ Thus, it will almost surely be necessary at least to extend the eccentric orbit-averaged code [30] to 2.5PN (and possibly 3PN) accuracy in the spins and 3PN in the non-spinning terms (as we show later) in order to obtain results that have errors $< 10^{-2}$. As discussed in [30], the extension of the orbit-averaged evolution to 3PN spinning terms just requires the extension of the quasi-Keplerian parametrization [32] for arbitrary spin orientations to 2.5PN, since the other ingredients are present in the literature. To extend this evolution to 3.5PN for non-spinning terms, one needs to compute the 3.5PN contributions to the orbit-averaged fluxes for eccentric binaries, which has not yet been done. However, the hybrid evolution code presented in this work already provides an improvement on the accuracy of the only precession-averaged eccentric evolution used in [19, 26], since we find that the differences in cosine tilts estimated from the only precession-averaged and hybrid evolutions can approach unity for some binaries. In addition to studying the accuracy of the code, we also use it to illustrate how eccentricity affects the tilts at infinity and perform some initial investigations into how well the tilts at infinity approximate those at formation in cases where eccentricity is not negligible.

The rest of the paper is organized as follows: In Sec. II, we introduce the orbital and spin parameters for an eccentric, precessing BBH, and provide details about the evolution equa-

¹ We use the standard PN order counting where n PN corresponds to terms of order $(v/c)^{2n}$ beyond leading order (v is the binary's orbital velocity), except for the precession equations, where the order counting is such that the leading spin-orbit term appears at 1.5PN as it does in the binary's orbital dynamics.

tions we use. In Sec. III, we discuss how we interface orbit-averaged and precession-averaged evolution equations to create a unified code to compute the tilts at infinity for precessing BBHs on eccentric orbits, and present various checks of the accuracy of the results. In Sec. IV, we discuss the effects of eccentricity on the tilts at infinity, and compare the hybrid evolution with purely precession-averaged evolution. Then in Sec. V we give examples of where the spin tilts at infinity are good and poor approximations to those at formation of the binary. Finally, we summarize and conclude in Sec. VI. We give an example usage of the code in Appendix A and derive a bound on the change in tilts between eccentricities close to 1 and the limiting value of 1 in Appendix B. We use geometrized ($G = c = 1$) units, and express all angles in radians throughout this paper.

II. ORBITAL AND SPIN EVOLUTION

A. Orbit-averaged evolution

Here, we discuss the parameters used to describe the orbital motion and spin-precession of eccentric BBHs, as reviewed in Sec. II of [30]. We first discuss the orbital dynamics. Let us consider a BBH with black hole masses m_1 and m_2 , mass ratio $q = m_2/m_1 \leq 1$, total mass $M = m_1 + m_2$, and dimensionless spin magnitudes of χ_1 and χ_2 . The spin orientations are determined by the tilt angles $\theta_{1,2} \in [0, \pi]$ between each spin and the binary's orbital angular momentum as well as the azimuthal angles $\psi_{1,2} \in [0, 2\pi)$ between the projections of the spin vectors onto the orbital plane and the binary's line of periastron (see Fig. 1 in [30] for a visual representation of these angles and orbital elements). We use the quasi-Keplerian parameterization of the binary's orbital motion, which we express in terms of an average orbital frequency ω and the temporal eccentricity e_t . (We will refer to this eccentricity as just e for the remainder of the paper, except where we want to emphasize its specific definition.) We also use the orbit-averaged dissipative dynamics (from radiation reaction) and spin-precession equations. Specifically, for the nonspinning terms, we use the 3PN computations from [33, 34] (the highest order for which the dissipative dynamics have been computed), along with the high-accuracy hyperasymptotic expansions for the eccentricity enhancement functions in the energy and angular momentum fluxes from Loutrel and Yunes [35]. The spinning contributions to the orbital dynamics are the 2PN expressions from [36, 37], the highest order to which this has been computed for arbitrary spin orientations (so we are including the leading-order spin-orbit and spin-spin interactions). The spin-precession equations (from [38]) are also 2PN accurate. In all of these expressions, the spin-induced quadrupole moments are specialized to their black hole values. The code [30] to evolve orbit-averaged evolution makes various internal consistency checks that the PN equations are not obviously incorrect (listed in Table I of [30]) and some of these can be triggered when evolving backwards in the hybrid evolution to compute the tilts at infinity, particularly due to the large eccentricities one obtains, as we will discuss later.

B. Precession-averaged evolution

To efficiently evolve BBHs over long timescales, [39, 40] introduced the precession-averaged approach. In particular, this allows one to compute the tilt angles at infinity (specifically infinite orbital angular momentum), which are well-defined except in the exactly equal-mass case, where the tilts do not approach a single value in that limit (see, e.g., the discussion in Sec. III A of [20] as well as [41]). The precession-averaged approximation relies on the precession timescale being much smaller than the radiation reaction timescale and is only 1PN accurate in the dissipative dynamics, as discussed in [40]. Thus, the precession-averaged dynamics lose accuracy close to the BBH merger, where we instead use the orbit-averaged evolution.

As discussed in Sec. II A of [20], following [42], if one just wants to compute the tilts at infinity for eccentric binaries, there is no change to the precession-averaged equations compared to the quasicircular case. (Of course, the eccentricity increases rapidly when evolving backwards, so the orbit averaging that underlies the precession-averaged evolution will become less accurate, due to the significant difference in orbital speeds at periastron and apoastron. However, this caveat also applies to the orbit-averaged equations we use.) Thus, we use the same precession-averaged code as in [20]. The only difference compared to the quasicircular case is that we use the eccentric expression for the magnitude of the orbital angular momentum to initialize the precession-averaged evolution. Here we use the Newtonian order expression, since this is what enters into the 2PN precession equations used in the orbit-averaged evolution:

$$L = m_1 m_2 \frac{\sqrt{1 - e^2}}{v}, \quad (1)$$

where $v = (M\omega)^{1/3}$ is the orbital velocity corresponding to the orbit-averaged orbital angular frequency ω (as used in the orbit-averaged code [30]).

III. INTERFACING ORBIT-AVERAGED AND PRECESSION-AVERAGED EVOLUTIONS

A key element of the hybrid method we use is determining the transition orbital velocity v_{trans} where we change from using orbit-averaged to precession-averaged evolution equations. Since the orbital velocity varies over an orbit in the eccentric case, even with just the conservative dynamics, we use the orbital velocity obtained from the orbit-averaged angular velocity to set the transition orbital velocity. The specific value of v_{trans} one uses depends on the accuracy one requires for the resulting tilts at infinity. The quasicircular hybrid evolution code in [20] uses a v_{trans} value obtained by demanding an accuracy of better than 10^{-3} in the cosines of the tilts at infinity, motivated by the expected measurement accuracy with next-generation GW detectors. While one might expect that the appropriate v_{trans} in the eccentric case would depend on the eccentricity, we find that using the quasicircular v_{trans} gives acceptable accuracy in the eccentric case.

The transition velocity in the quasicircular case is given by

$$v_{\text{trans}} = -0.05q^2 + 0.06. \quad (2)$$

In the quasicircular case, the ($m = 2$ mode) GW frequency is given by $f_{\text{trans}} = v_{\text{trans}}^3/(\pi M)$. We use the same expression in the eccentric case, since the orbit-averaged code sets $f_{\text{GW}} = \omega/\pi$, where ω is the orbit-averaged orbital frequency. Thus, we are determining the transition point in terms of the orbit-averaged orbital frequency, as mentioned above. To validate their v_{trans} on systems outside the training sample, [20] generated a synthetic set of 500 binary systems, with parameters drawn from the following ranges: $m_1, m_2 \in [5, 100]M_\odot$; $\chi_1, \chi_2 \in [0, 1]$; $\theta_1, \theta_2 \in [0, \pi]$; $\phi_{12} \in [0, 2\pi]$; with a reference frequency $f_{\text{ref}} = 20$ Hz. For each binary, they computed the absolute difference in $\cos \theta_A^\infty$ ($A \in \{1, 2\}$) obtained using the v_{trans} [from Eq. (2)] and $0.6v_{\text{trans}}$. They used $0.6v_{\text{trans}}$ instead of the obvious choice of $0.5v_{\text{trans}}$ because of the computational cost of using the lower velocity, especially for nearly equal-mass binaries, with the earlier, less efficient version of the code. The results, summarized in Fig. 6 in [20], show that the difference in $\cos \theta_A^\infty$ for all 500 systems are below 10^{-3} , thus validating their choice of v_{trans} . However, in our case, we use the natural choice of $0.5v_{\text{trans}}$, since we find that it is possible to evolve to $0.5v_{\text{trans}}$ in a reasonable amount of time, without incurring any hardware memory issues (which was the case in quasicircular code from [20] for close to equal mass binaries). We also have a much larger sample set of 2000 simulated BBHs to test our code, because we are sampling more input parameters, namely the orbital eccentricity as well as both ψ_1 and ψ_2 (instead of just ϕ_{12}).

A. Validating v_{trans}

To validate that the quasicircular v_{trans} indeed gives sufficient accuracy in the eccentric case, we now carry out the same convergence test performed in [20] to validate v_{trans} [given by Eq. (2)], except that we are now using v_{trans} and $0.5v_{\text{trans}}$ as our two transition velocities. Using these two transition velocities, we measure $\delta \cos \theta_1^\infty$ and $\delta \cos \theta_2^\infty$, which denote the difference in cosines of spin tilt 1 and spin tilt 2 at infinity for the primary and secondary black holes, respectively. However, as mentioned in the introduction, instead of demanding the same accuracy in the cosines of the tilts at infinity as in the quasicircular case, we instead only require an accuracy of better than 10^{-2} , since the orbit-averaged eccentric equations we use are less accurate than the quasicircular ones (2PN in spinning terms and 3PN in nonspinning terms in the eccentric code compared to 3PN in spinning terms and 3.5PN in nonspinning terms in the quasicircular code). In fact, we expect that we have errors of up to ~ 0.1 from the lack of 2.5PN spin terms and 3.5PN nonspinning terms, given the results in the quasicircular case (see Fig. 7 in [20] for the spin terms and the discussion later for the nonspinning terms). Nevertheless, we keep 10^{-2} as our desired tolerance, since it is below the anticipated statistical errors for observations in the fifth observing run of the advanced GW detector network [23]. Thus, along with the results in the quasicircular

case, this suggests that once we have the 2.5PN spin terms and 3.5PN nonspinning terms in the orbit-averaged evolution equations, the v_{trans} we are using, or a scaling of it to slightly smaller values would give an error of $< 10^{-2}$. Ref. [20] also considered the difference in the tilts at infinity between the 2.5PN and 3PN spin terms and found that these are at most $\sim 10^{-2}$, so to ensure that the errors are $< 10^{-2}$, one will want to extend the orbit-averaged evolution to at least 3PN in the spinning terms. As discussed in [30], obtaining the orbit-averaged evolution at 3PN only requires extending the quasi-Keplerian parameterization for arbitrary spins to 3PN—all the other ingredients are already available in the literature.

To validate v_{trans} , we analyze a total of 2000 binaries, with parameters spanning a broad range, only differing with respect to the distribution used in the quasicircular analysis [20] in sampling the spin angles, where we sample the spin angles uniformly on the 2-sphere, rather than uniformly in the tilt angles, as in the quasicircular case, and also sample both the ψ_1 and ψ_2 angles, since both enter into the orbit-averaged eccentric evolution, rather than just ϕ_{12} , which is all that is necessary in the quasicircular case. The reference frequency f_{ref} is fixed at 20 Hz, with initial eccentricities $e_{20 \text{ Hz}}$ uniformly distributed between 0 and 0.7. We restrict the maximum eccentricity to 0.7 for all the analyses in this paper because evolving backward from higher starting eccentricities triggered some of the checks that the PN equations we are using are not reliable at the initial conditions for many binaries. Specifically, the checks that commonly fail for $e_{20 \text{ Hz}} > 0.7$ are those checking that the binary is bound (i.e., that its energy is negative), that the binary's energy is increasing as the binary evolves backward (i.e., the time derivative of the binary's energy is negative), and that the PN expansion parameter $\bar{x} = v^2/(1 - e^2) < 1$.

In Fig. 1, we show the same convergence test as in the quasicircular case for the 1963 binaries out of the 2000 binaries for which the orbit-averaged evolution reaches a stopping frequency of f_{stop} which is within 1% of the f_{trans} associated with $0.5v_{\text{trans}}$ (corresponding to a v_{stop} within 0.033% of the value of $0.5v_{\text{trans}}$), without triggering any stopping condition. The maximum difference in $\cos \theta_1^\infty$ is 5.37×10^{-3} , corresponding to $m_1 = 17.49M_\odot$, $m_2 = 15.69M_\odot$, $\chi_1 = 0.081$, $\chi_2 = 0.847$, $\theta_1 = 1.852$, $\theta_2 = 2.395$, $\psi_1 = 4.460$, $\psi_2 = 0.257$ and $e_{20 \text{ Hz}} = 0.063$. The $\delta \cos \theta_2^\infty$ for this binary is 5.68×10^{-4} . On the other hand, the maximum difference in $\cos \theta_2^\infty$ is 4.30×10^{-3} , corresponding to $m_1 = 29.23M_\odot$, $m_2 = 16.94M_\odot$, $\chi_1 = 0.965$, $\chi_2 = 0.580$, $\theta_1 = 0.887$, $\theta_2 = 1.654$, $\psi_1 = 5.607$, $\psi_2 = 2.697$ and $e_{20 \text{ Hz}} = 0.138$. The $\delta \cos \theta_1^\infty$ for this binary is 1.50×10^{-3} . We also plot the eccentricity at v_{trans} in Fig. 2, where we find that most of them are greater than 0.9, and some are even greater than 0.999. Since the orbit-averaged approximation is less accurate for large eccentricities, future work will check the accuracy of the approximation by comparing the evolutions with and without orbit averaging.

We now discuss the binaries for which the orbit-averaged evolution stopped before reaching v_{trans} . This is because of different stopping conditions implemented in the orbit-averaged code to ensure that the equations we are evolving do

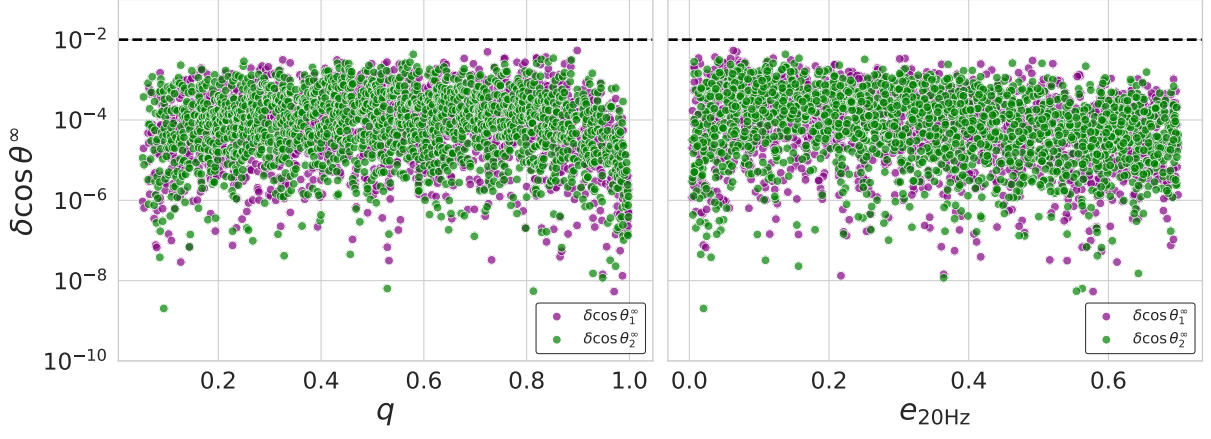


FIG. 1. Absolute values of the differences in cosines of spin tilts obtained using v_{trans} and $0.5v_{\text{trans}}$ as the transition orbital velocities. This plot restricts to the 1963 binaries that reach $0.5v_{\text{trans}}$ without the orbit-averaged evolution triggering a stopping condition. We plot these versus mass ratio on the left and eccentricity (at 20 Hz) on the right. All the differences are well below our desired tolerance of 10^{-2} .

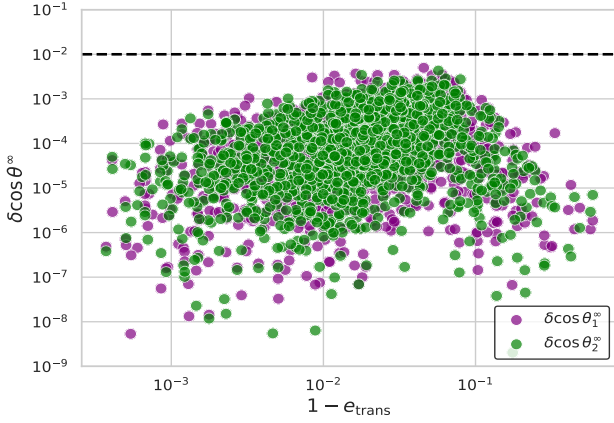


FIG. 2. The differences in the cosine of spin tilts at infinity computed using transition velocities of v_{trans} and $0.5v_{\text{trans}}$ versus the eccentricities at transition, for the 1963 binaries which successfully evolved to $0.5v_{\text{trans}}$. Most of the eccentricities at transition are greater than 0.9 and the distribution extends to above 0.999.

not give obviously unphysical results at initial or any stage of the evolution. Specifically, we consider the 9 binaries whose GW frequency when the evolution stopped differs from the desired f_{trans} by more than 1% (i.e., the final orbital velocity reached differs from the desired v_{trans} by more than $\sim 0.3\%$). All these binaries had an initial eccentricity of $e_{20\text{ Hz}} < 0.004$, which is smaller than that allowed by the orbit-averaged evolution equations. This is because, due to the 2PN spin-spin contributions to \dot{e}_t^2 , eccentric, precessing binaries attain a minimum, non-zero value of e_t when evolved forward. This causes e_t^2 to become negative when evolving backwards (see the discussion in [30, 36, 37]). We find that the check that $\dot{\omega} \leq 0$ gets triggered by the interpolated data points in these cases, but the integration is stopped because $e_t^2 < 0$. On the other hand, all the 1963 binaries which stopped within 1%

of f_{trans} , stopped due to the evolution reaching the desired ending frequency. Finally, 25 binaries were not able to start their evolution because their initial conditions corresponded to a positive energy (i.e., the binary is not bound), and one binary did not evolve because the orbital angular momentum was not increasing when evolving backward in time (i.e., its time derivative is positive), at the initial conditions.

For binaries that stop their evolution before reaching within 1% of f_{trans} , we start the precession-averaged evolution at the stopping frequency f_{stop} . Since this is above the desired transition frequency, we expect that the tilts at infinity will be less accurate than if we had been able to evolve to the desired frequency f_{trans} . To estimate how much accuracy we lose in such cases, we compare with the tilts at infinity obtained when transitioning to the precession-averaged evolution at $2v_{\text{stop}}$. Since we are comparing with an earlier transition point, where the precession-averaged evolution will be less accurate, this gives an upper bound on the size of the errors. We notice that we are only able to evolve only 1 out of 9 binaries because most of them stopped very early in their evolutions (stopping frequencies between 15 and 20 Hz), thus a transition velocity of $2v_{\text{stop}}$ would correspond to a frequency higher than $f_{\text{ref}} = 20\text{ Hz}$. This binary has the parameters $m_1 = 75.32M_\odot$, $m_2 = 63.33M_\odot$, $\chi_1 = 0.959$, $\chi_2 = 0.137$, $\theta_1 = 2.399$, $\theta_2 = 0.499$, $\psi_1 = 0.898$, and $\psi_2 = 4.549$ and $e_{20\text{ Hz}} = 0.004$. We find that the difference in cosine of tilt 1 is 2.5×10^{-3} , while that in tilt 2 is 2.1×10^{-2} . This shows that one still gets good accuracy from the hybrid evolution in most cases, even if the orbit-averaged evolution is not able to reach the desired transition frequency.

We also compare the differences we get in the cosines of the tilts at infinity obtained using the 2.5PN and 3PN nonspinning terms in the orbit-averaged evolution in Fig. 3. Out of the total 1963 binaries which successfully evolved to v_{trans} with both orders of the nonspinning terms, 236 binaries have $\delta \cos \theta_1^\infty > 10^{-2}$, while 226 binaries have $\delta \cos \theta_2^\infty > 10^{-2}$. We find the same binary produced both the maximum $\delta \cos \theta_1^\infty$ and $\delta \cos \theta_2^\infty$ values, which are 1.3×10^{-3} and 7.9×10^{-2} , re-

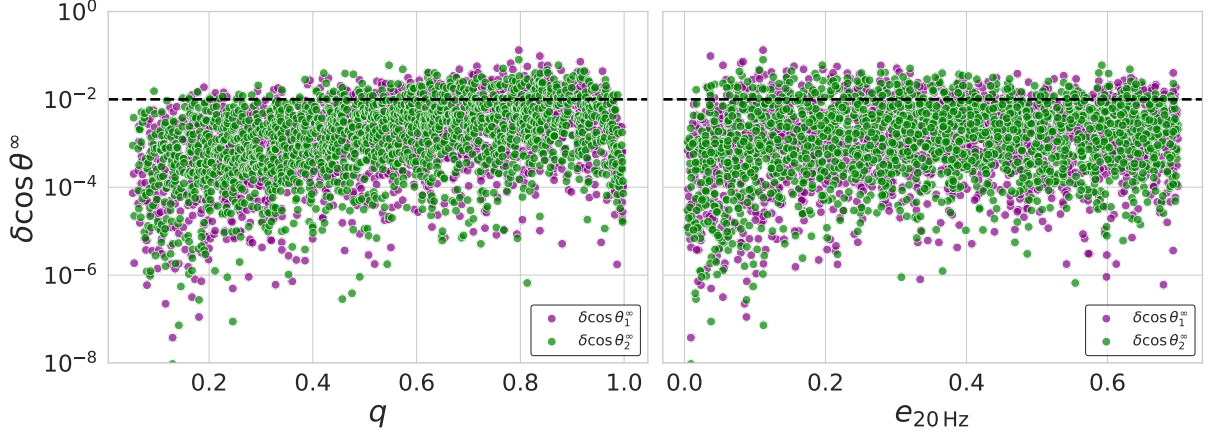


FIG. 3. The differences in the cosine of spin tilts at infinity computed using 2.5PN and 3PN nonspinning terms in the orbit-averaged evolution, versus mass ratio (left) and eccentricity at 20 Hz (right) for the 1963 binaries which successfully evolved to v_{trans} using both evolutions. About 10% of the binaries have differences greater than 10^{-2} , though we expect that this overestimates the errors from the 3PN truncation in the nonspinning terms used by default.

spectively. The binary parameters are $m_1 = 78.97M_\odot$, $m_2 = 99.10M_\odot$, $\chi_1 = 0.651$, $\chi_2 = 0.857$, $\theta_1 = 2.526$, $\theta_2 = 0.564$, $\psi_1 = 1.125$, $\psi_2 = 0.140$, and $e_{20\text{Hz}} = 0.112$.

Since [20] did not check the differences due to the PN order of the nonspinning terms, we perform this analysis for quasicircular binaries using the default PN approximant (TaylorT5) in the orbit-averaged evolution.² (This uses the same 1963 binaries used in the eccentric case with the eccentricity set to zero.) Here the maximum differences in the cosines of the tilts at infinity between 3PN and 3.5PN (the highest two orders available in the quasicircular code) are $\delta \cos \theta_1^\infty = 3.5 \times 10^{-3}$ and $\delta \cos \theta_2^\infty = 3.3 \times 10^{-3}$. These are somewhat above the desired tolerance of 10^{-3} for the quasicircular code, but we expect that these differences provide an upper bound on the errors due to using the 3.5PN evolution equations, which are likely at most around 10^{-3} , since the maximum differences when using the 2.5PN and 3PN nonspinning terms are a factor of ~ 2 larger (8.4×10^{-3} and 7.8×10^{-3} , respectively). We leave an explicit comparison with the 4PN and 4.5PN nonspinning terms from [43] for future work. To enable a direct comparison of the eccentric evolution (which uses TaylorT4) with the quasicircular evolution, we compute the differences between the 2.5PN and 3PN nonspinning terms for both the evolutions (using the TaylorT4 approximant for quasicircular evolution). We find that $\delta \cos \theta_1^\infty = 2.3 \times 10^{-2}$ and $\delta \cos \theta_2^\infty = 2.5 \times 10^{-2}$. Thus, since the differences between 3PN and 3.5PN with TaylorT4 in quasicircular evolution are 6.7×10^{-3} and 3.3×10^{-3} , respectively, it is likely that the errors due to the truncation at 3PN for the nonspinning terms in the eccentric case are a few times 10^{-2} . (This is obtained by computing the ratio of the differences between 3PN and 3.5PN to those between 2.5PN and 3PN in the quasicircular

case and then multiplying by the differences between 2.5PN and 3PN in the eccentric case.)

B. Analysis for very high eccentricities

Apart from the results in Fig. 1 where initial eccentricity was varied from 0 to 0.7, we also evolved 1000 highly eccentric binaries, where $e_{20\text{Hz}}$ ranged from 0.7 to 0.99, and all other parameters are sampled from the ranges defined in earlier sections. Only 166 of these binaries successfully completed their evolution. The other 834 of them were not able to start their evolution because one of the internal consistency checks of the PN expressions failed for the initial conditions. For most of the binaries (697), the problem was that the PN energy expression used in the evolution gave an unbound binary, while many others (134 binaries) had $\bar{x} \geq 1$ initially, so we do not trust the PN equations we use. For one of the binaries, the initial value of the energy time derivative is positive (while it should be negative due to GW emission), while for the other two binaries this time derivative becomes positive during the evolution. For the 166 binaries which evolved successfully to v_{trans} , they were successfully able to evolve to $0.5v_{\text{trans}}$ and we found that the differences are all lower than our desired 10^{-2} tolerance.

C. Runtime

For our 1963 successful binaries, we calculated the time it takes to compute the spin tilts at infinity using our hybrid evolution code, averaging over 5 evolutions for each binary. These tests were performed on a heterogeneous computing pool with a variety of CPUs, including Intel's Skylake-X (2017) and more recent models, as well as AMD's Zen 4 (2022) and later generations, with base clock speeds ranging

² The TaylorTX approximant is referred to as `SpinTaylorTX` in the quasicircular code, for consistency with the waveform models in LALSuite.

between 2.2 GHz and 4.7 GHz. The results are presented in Fig. 4.

The eccentric hybrid evolution code runtimes are roughly in the same range as those obtained using the quasicircular hybrid evolution code (see Fig. 10 in [20]), though they are smaller for larger eccentricities, where the binary's physical evolution is quicker. This is why as the mass ratio approaches 1, the eccentric code becomes faster than the quasicircular code for the vast majority of BBHs which we consider.

IV. COMPARISON WITH OTHER TYPES OF EVOLUTIONS

A. Comparison with quasicircular evolution

Here we illustrate that there are portions of parameter space where eccentricity has a significant effect on the tilts at infinity. We do this by comparing the results of the eccentric hybrid evolution with the quasicircular hybrid evolution (from [20]) applied to the set of the 1963 binaries which successfully evolved to v_{trans} (where we just ignore the eccentricity when applying the quasicircular code). We use the same PN orders (3PN nonspinning and 2PN spinning) for the quasicircular evolution as are used in the eccentric evolution, as well as the same approximant (TaylorT4), for an exact comparison. We show the differences in Fig. 5, where we find that 542 binaries have $\delta \cos \theta_1^\infty \geq 10^{-2}$, and an equal number of binaries have $\delta \cos \theta_2^\infty \geq 10^{-2}$. These differences are similar to or greater than unity in a few cases. The maximum difference obtained for cosine of tilt 1 was $\delta \cos \theta_1^\infty = 5.97 \times 10^{-1}$ for the binary with $m_1 = 95.90 M_\odot$, $m_2 = 77.72 M_\odot$, $\chi_1 = 0.212$, $\chi_2 = 0.972$, $\theta_1 = 0.161$, $\theta_2 = 2.535$, $\psi_1 = 0.519$, $\psi_2 = 4.912$, and $e_{20 \text{ Hz}} = 0.512$, with corresponding $\delta \cos \theta_2^\infty = 1.61 \times 10^{-3}$. The maximum cosine tilt 2 difference was $\delta \cos \theta_2^\infty = 1.75$ for the binary with $m_1 = 48.39 M_\odot$, $m_2 = 45.78 M_\odot$, $\chi_1 = 0.289$, $\chi_2 = 0.003$, $\theta_1 = 0.067$, $\theta_2 = 2.834$, $\psi_1 = 4.956$, $\psi_2 = 6.219$, and $e_{20 \text{ Hz}} = 0.476$, with corresponding $\delta \cos \theta_1^\infty = 1.57 \times 10^{-1}$.

B. Hybrid evolution vs precession-averaged evolution

We now compare the tilts at infinity estimates from the only precession-averaged evolution and from the full hybrid evolution. We consider the same 1963 binaries which successfully evolved to v_{trans} from the 2000 binaries described earlier in Sec. III A, and show the results in Fig. 6. We observe that there are large differences ($\geq 10^{-1}$ and some approaching unity) in the spin tilts at infinity for a significant number of binaries, particularly for more symmetric mass binaries (q close to 1) and lower values of starting eccentricities. These maximum differences are significantly larger than those found for the quasicircular evolution, where the differences are $\lesssim 10^{-1}$ (see Fig. 8 in [20]). The comparison in [20] uses a higher-order PN expression to compute the initial orbital angular momentum for the only precession-averaged evolution than the 1PN one used in the hybrid evolution, since this is found to give

slightly better agreement between the two evolutions, while we just use the Newtonian expression used in the hybrid evolution here. However, the differences between the two evolutions in the quasicircular case are still only $\lesssim 10^{-1}$ when using the 1PN expression for the orbital angular momentum for the only precession-averaged evolution.

V. TILTS AT INFINITY VS TILTS AT FORMATION

As is discussed in Sec. I, the L for eccentric binaries is bounded from above, so there is necessarily a lower bound on the uncertainty in the tilts at formation for eccentric binaries, unlike the quasicircular case where this uncertainty can in principle be arbitrarily small. Nevertheless, the maximum L value attained for eccentric binaries (as $e \nearrow 1$) can still be large enough that there is minimal uncertainty in the tilts at formation. However, in other cases, particularly those with larger eccentricities at the reference frequency, there is a non-negligible uncertainty in the tilts at formation, and the tilts one obtains when evolving back to e values close to 1 with only orbit-averaged evolution will be a better approximation to the tilts at $e \nearrow 1$ than the tilts at infinity. Recall that for eccentric binaries, $e \nearrow 1$ corresponds to orbital separation being infinite, but a finite L , whereas the tilts at infinity are obtained in the limit where $L \rightarrow \infty$.

Here we give an example of an eccentric case where the tilts at infinity are not a particularly good approximation to the tilts at formation (differences above 10^{-2}) as well as a case where they are a better approximation. Here, we refer to the limit $e \nearrow 1$ as formation for ease of exposition, though we are not considering any particular astrophysical formation scenario. We also show how the tilts at infinity depend on the transition velocity as well as how the tilts at different transition points vary, for comparison with the same illustration in the quasicircular case in Fig. 5 of [20]. Specifically, Fig. 7 shows the behavior of the same BBH with two different starting eccentricities, $e_{20 \text{ Hz}} = 6.25 \times 10^{-3}$ (binary A) and $e_{20 \text{ Hz}} = 0.05$ (binary B). We chose the binary parameters quasi-randomly for this illustration, and they are $m_1 = 7.67 M_\odot$, $m_2 = 6.42 M_\odot$, $\chi_1 = 0.88$, $\chi_2 = 0.35$, $\theta_1 = 2.93$, $\theta_2 = 1.77$, $\psi_1 = 0$, and $\psi_2 = 4.25$, at a reference frequency of 20 Hz. We choose two starting eccentricities $e_{20 \text{ Hz}} = 6.25 \times 10^{-3}$ and 0.05, to contrast the different values of L/M^2 attainable as $e \nearrow 1$. We compute the L/M^2 values as $e \nearrow 1$ (denoted as $L_{e \nearrow 1}/M^2$) by evolving the binary backwards from f_{ref} to v_{trans} using orbit-averaged evolution and then using the leading-order expression from Eq. (5.11) in Peters [12] to compute the value in the limit $e \nearrow 1$; we have checked that evolving to $v_{\text{trans}}/2$ instead and then applying the Peters expression produces negligible differences. We find $L_{e \nearrow 1}/M^2$ to be 7.9 and 4.1 for binaries A and B, respectively. We thus expect the tilts at formation for binary A to have smaller intrinsic uncertainties than those for binary B, since the uncertainties in the tilts at a finite L go as M^2/L in the precession-averaged approximation [40]. As an illustration, we take the spin angles at the smallest value of $v_{\text{trans}} = 10^{-3}$ plotted in Fig. 7 and the $L_{e \nearrow 1}/M^2$ values, and use Eqs. (23) in [20] to obtain differ-

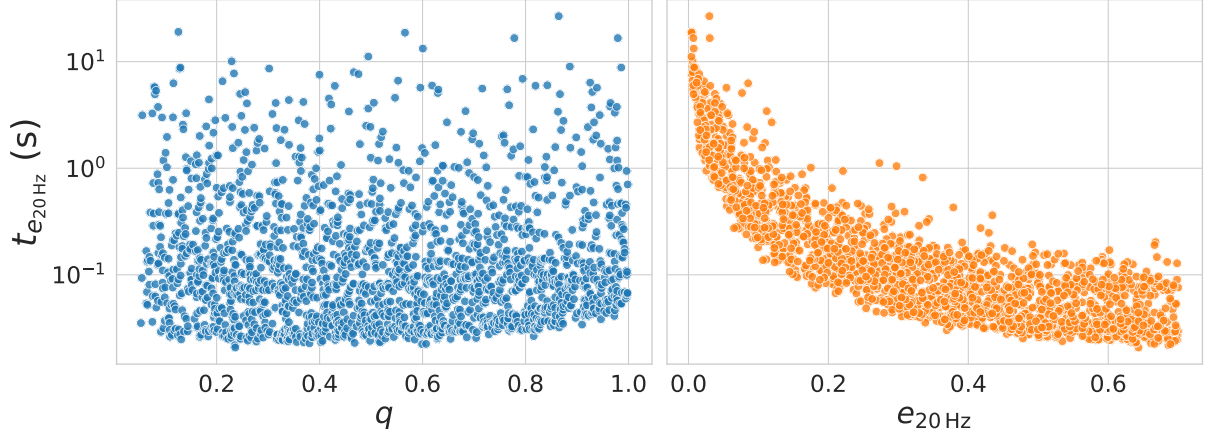


FIG. 4. The time taken by the eccentric hybrid evolution code to compute the spin tilts at infinity for each of 1963 binaries which successfully evolved to v_{trans} . We show the variation along with mass ratio q and starting eccentricity $e_{20\text{Hz}}$. There is a strong correlation observed between the runtime and $e_{20\text{Hz}}$, as binaries with larger starting eccentricities evolve more quickly (in physical time).

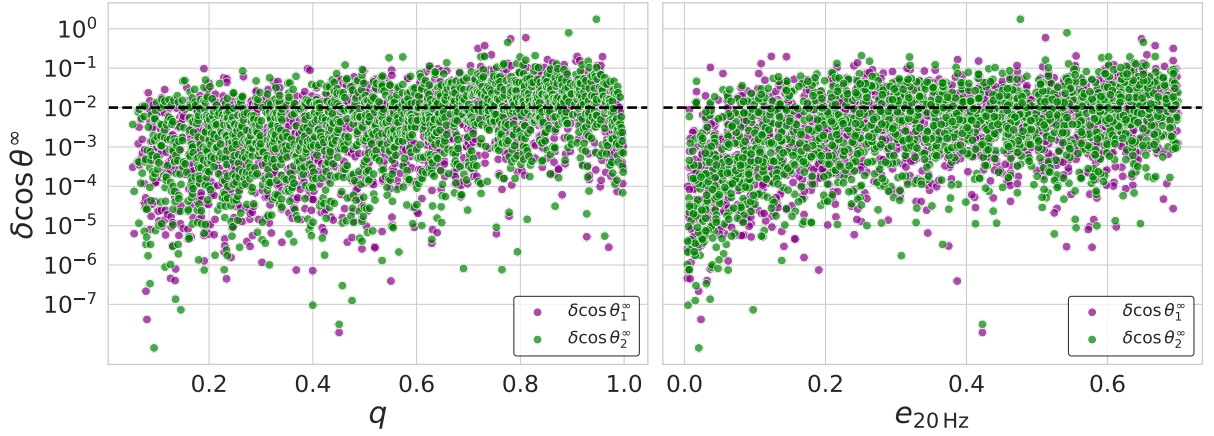


FIG. 5. The absolute values of the differences in the cosines of the spin tilts at infinity obtained using the eccentric hybrid evolution and the quasicircular evolution (taking the eccentricity to be zero and using the same PN orders as in the eccentric hybrid evolution), for the 1963 binaries which successfully evolved to v_{trans} .

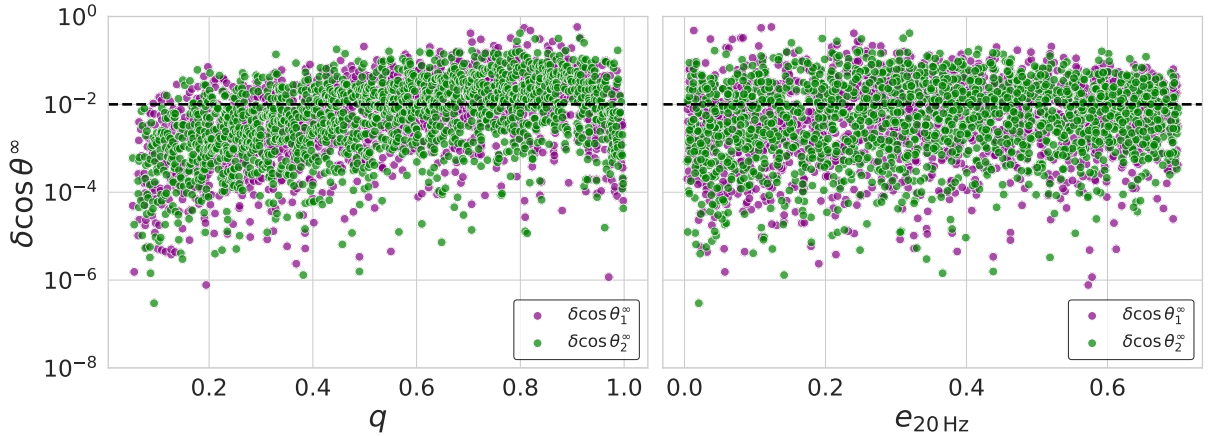


FIG. 6. The absolute values of the differences between the cosines of spin tilts at infinity computed using the hybrid evolution code and using only precession-averaged evolution, for the 1963 binaries which successfully evolved to v_{trans} . Some of the differences are much higher than 10^{-2} , and even close to 1 in some cases, showing the importance of using the hybrid evolution.

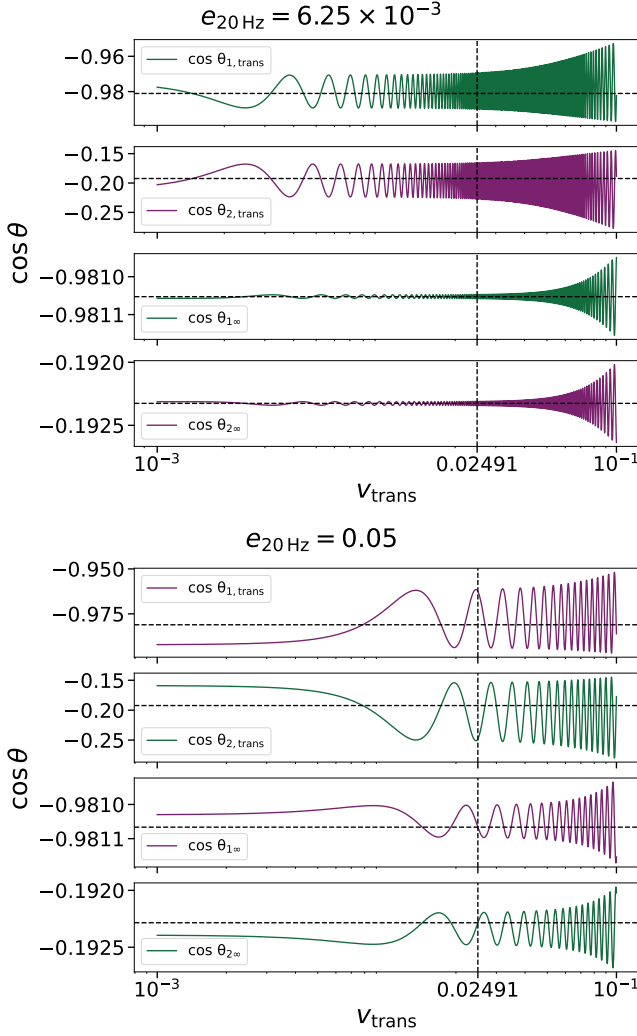


FIG. 7. Variation of spin tilts at transition and at infinity, with v_{trans} , for two different starting eccentricities ($e_{20\text{ Hz}} = 6.25 \times 10^{-3}$ and $e_{20\text{ Hz}} = 0.05$). All the other binary parameters are fixed to the values given in the text. The upper panels in each subfigure show the cosines of tilts at different v_{trans} values, while the lower panels show the cosines of spin tilts at infinity. The vertical dashed black line denotes the empirical value of the v_{trans} [from Eq. (2)], while the horizontal dashed black line denotes the tilts at infinity computed using that empirical v_{trans} .

ences in the cosines of tilt 1 and tilt 2 over a precessional cycle of 0.02, 0.06 for binary A and 0.03, 0.09 for binary B.

However, we see a notable difference in the behavior of the tilts at small values of v_{trans} in Fig. 7. While in both cases, the tilts at infinity approach a constant value, for binary A, the tilts at small values of v_{trans} still seem to be oscillating around the tilts at infinity, while for binary B they have apparently asymptoted to constants different from the tilts at infinity (differences of 0.01 and 0.03 for tilts 1 and 2, respectively). We can show that there is no significant evolution of the tilts for binary B between $v_{\text{trans}} = 10^{-3}$ and 0 using the bounds derived in Appendix B, where the eccentricity of binary B is 0.999863 at $v_{\text{trans}} = 10^{-3}$. The maximum absolute difference

in cosine tilt 1 and 2 values to $v_{\text{trans}} = 0$ is 1.1×10^{-3} and 4.9×10^{-3} . These are more than 6 times smaller than the differences compared to the tilts at infinity. However, for the eccentricity of binary A of 0.999490 at $v_{\text{trans}} = 10^{-3}$, those upper bounds are 0.015 and 0.065,³ which are larger than the tilt differences between $v_{\text{trans}} = 10^{-3}$ and at infinity (4×10^{-3} and 0.01, respectively, for tilts 1 and 2). Future work will consider if these conclusions change significantly when evolving without orbit averaging, and if they do not (at least for some binaries). If there is not a significant change to these conclusions, then we will also determine where in the eccentric parameter space it is better to compute the tilts at infinity as a proxy for the tilts at formation (as for binary A) and where it is better to evolve backwards using just the orbit-averaged evolution to estimate the tilts at formation (as for binary B).

VI. SUMMARY AND FUTURE DIRECTIONS

This paper presents the first public hybrid evolution code for eccentric, precessing BBHs to compute tilts at infinity and studies its accuracy. The hybrid evolution approach we employ uses both orbit-averaging and precession-averaging at different orbital separations, transitioning between the two at an empirically determined transition orbital velocity v_{trans} , to evolve BBHs from a reference frequency backwards in time to compute tilts at infinity. We have shown that there are significant differences (up to order unity) in the cosines of spin tilts obtained using our hybrid evolution compared to the only-precession-averaged evolution that has been used in [19], which already showed that neglecting a small but non-zero residual eccentricity in the detectors' band ($e_{10\text{ Hz}} \leq 0.05$), can lead to significant biases once the binary is evolved backwards to a large separation ($\sim 10^4 M$). Our code is public [31], and it will be part of LALSuite after being reviewed, so it can be used for such studies. Additionally, our code can be used to compute the tilts at infinity when analyzing compact binary GW signals using an eccentric, precessing BBH waveform model (which have started to be developed [44, 45]), though some work will be necessary to convert the eccentricity definition used in the cited waveform models to the eccentricity definition used in our code.

With the differences in cosines of spin tilts at infinity lower than $\sim 10^{-2}$, we have shown that the transition orbital velocity v_{trans} used in the quasicircular hybrid evolution in [20] produces acceptable accuracy in the tilts at infinity for eccentric cases. These differences are lower than the anticipated statistical uncertainties in the fifth observing run of the advanced GW detector network. However, given the checks we made of the accuracy of this code and the quasicircular one, we also expect that it will be necessary to extend the eccentric orbit-averaged evolution from its current 2PN accuracy in spinning terms and 3PN accuracy in nonspinning terms to

³ Likely not coincidentally, the upper bounds in this case are quite similar to the differences in the cosines of the tilts over a precessional cycle for this binary.

3PN and 3.5PN, respectively, to obtain an overall accuracy of $< 10^{-2}$. Additionally, it will be necessary to check the accuracy of our orbit-averaged evolution against an evolution without orbit averaging, particularly since the backwards evolution leads to large eccentricities, where orbit averaging becomes less accurate, due to the large difference between orbital velocities at periastron and apastron. Possibilities for evolution without orbit averaging include direct integration of the PN equations of motion, without using the quasi-Keplerian formulation, as in [46]; osculating orbits, as in [47, 48] (though these do not include spin contributions); or by extending the closed-form solution to the 1.5PN non-dissipative dynamics from [49] to incorporate the effect of radiation reaction (and possibly higher-order terms) using perturbation theory. Additionally, one will need further improvements to the accuracy of the hybrid evolution for it to be below the statistical errors anticipated for third generation ground-based detectors like Einstein Telescope and Cosmic Explorer as well as space-based detectors like LISA, with their expected exquisite sensitivity.

We also have illustrated how the tilts at infinity are not always a good approximation to the tilts obtained when evolving back to $e \nearrow 1$ in eccentric cases, and that the tilts obtained when evolving backwards to a finite separation may be a better approximation, at least when evolving with orbit averaging. If this conclusion holds when evolving without orbit averaging, future work will generalize the bounds on the difference between the tilts at a high eccentricity and $e \nearrow 1$ that we derived here for orbit-averaged case to the case without orbit averaging and (if possible) sharpen it. We will then use these bounds to determine where in parameter space it is better to compute the tilts at infinity as a proxy for the tilts at formation for eccentric, precessing BBHs and where one should just evolve backwards to a finite separation (and what separation to evolve backwards to, to obtain a given accuracy).

ACKNOWLEDGMENTS

We thank Matthew Mould for useful comments on the manuscript. AS is supported by NSF grant PHY-2308887. NKJ-M is supported by NSF grant AST-2205920. AG is supported in part by NSF grants PHY-2308887 and AST-2205920. KSP acknowledges support from STFC grant ST/V005677/1. The authors are grateful for computational resources provided by the LIGO Laboratory and supported by National Science Foundation Grants PHY-0757058 and PHY-0823459. This study used the software packages LALSuite [29], matplotlib [50], numpy [51], pandas [52], and scipy [53].

This is LIGO document number P2500251.

Appendix A: Example usage of code

TABLE I. Examples of using the code [31] introduced in this paper to evolve eccentric, precessing BBHs, starting from a reference frequency of 20 Hz, all the way to infinity, in an interactive Python session, using the highest PN order expressions available.

```
# Setup
>>> from lalsimulation.tilts_at_infinity import prec_avg_tilt_comp, calc_tilts_at_infty_hybrid_evolve
>>> from lal import MSUN_SI
>>> m1, m2 = 50., 45. # solar masses
>>> chi1, chi2 = 0.8, 0.6
>>> tilt1, tilt2, psi1, psi2 = 1.3, 0.4, 0.6, 2.7 # rad
>>> phi12 = psi2 - psi1 #relative azimuthal angle
>>> f0 = 20. # Hz
>>> e0 = 0.3 # starting eccentricity at 20 Hz

# Calculate spin tilts at infinity
# For only precession-averaged evolution
>>> prec_avg_tilt_comp(m1*MSUN_SI, m2*MSUN_SI, chi1, chi2, tilt1, tilt2, phi12, f0, e0)
{'tilt1_inf': 1.1104672438023913, 'tilt2_inf': 0.8510182154945696}

# The same through the hybrid evolution interface
>>> calc_tilts_at_infty_hybrid_evolve(m1*MSUN_SI, m2*MSUN_SI, chi1, chi2, tilt1, tilt2, phi12, f0, psi1,
e0, prec_only=True)
{'tilt1_inf': 1.1104672438023913, 'tilt2_inf': 0.8510182154945696, 'tilt1_f_stop': None,
'tilt2_f_stop': None, 'phi12_f_stop': None, 'f_stop': None, 'eccentricity_f_stop': None}

# For hybrid evolution
>>> calc_tilts_at_infty_hybrid_evolve(m1*MSUN_SI, m2*MSUN_SI, chi1, chi2, tilt1, tilt2, phi12, f0, psi1,
eccentricity=e0)
{'tilt1_inf': 1.1765971973318956, 'tilt2_inf': 0.7252032198568954, 'tilt1_f_stop': 1.276168597718065,
'tilt2_f_stop': 0.47964766389584523, 'phi12_f_stop': 4.1728009459579205, 'f_stop':
0.0050440712586374776,
'eccentricity_f_stop': 0.9960631317641313}

# Sometimes the orbit-averaged code will not be able to evolve to the desired empirical f_trans
# In this case, the precession-averaged evolution starts from the frequency at which the orbit-averaged
code stopped.

>>> e0 = 0.001 # Eccentricity for this test case

# Use verbose=True to get more details of the evolution
>>> calc_tilts_at_infty_hybrid_evolve(m1*MSUN_SI, m2*MSUN_SI, chi1, chi2, tilt1, tilt2, phi12, f0, psi1,
eccentricity=e0, verbose=True)

RuntimeWarning: The evolution stopped at f_stop = 19.695466447044392 Hz. This is outside the allowed 1%
tolerance around the empirical transition frequency 0.005044066816799267 Hz. Starting the precession-
averaged evolution from f_stop. Accuracy in spin tilts at infinity will be reduced if the stopping
frequency is significantly higher than the desired transition frequency.
The tilts at f_stop are: tilt1 = 1.30404788878423, tilt2 = 0.38488248446149187, phi12 = 2.106964977851078
and eccentricity is 1.4523807720004001e-05
{'tilt1_inf': 1.118011978527311, 'tilt2_inf': 0.8375968780052747, 'tilt1_f_stop': 1.30404788878423,
'tilt2_f_stop': 0.38488248446149187, 'phi12_f_stop': 2.106964977851078, 'f_stop':
19.695466447044392,
'eccentricity_f_stop': 1.4523807720004001e-05}
```

Here, we illustrate the use of our eccentric hybrid evolution code with some examples. The function `calc_tilts_at_infty_hybrid_evolve()` computes the tilts at infinity for a BBH using hybrid evolution. The mandatory inputs to this function are as follows (with the binary parameters all in SI units): m_1 , m_2 , χ_1 , χ_2 , θ_1 , θ_2 , ϕ_{12} , and f_{ref} . Here, m_1 and m_2 represent the masses

of primary and secondary black holes respectively, while $\chi_{1,2}$ represent the dimensionless spin magnitudes. The spin angles are represented by $\theta_{1,2}$ (spin tilt angles) and ϕ_{12} (the relative azimuthal angle), while f_{ref} denotes the GW frequency to start the evolution with, where this is defined in the orbit-averaged way discussed in [30]. Optional keyword arguments for the function include ψ_1 , e_0 (the

binary's eccentricity at f_{ref}), `spin0`, and `phase0`, where the default values for the first two are 0 and for the second two are None, which corresponds to the maximum value available. Here `spin0` and `phase0` denote twice the PN order of spinning terms and nonspinning terms, respectively, in the orbit-averaged evolution equations. For eccentric evolution, the only allowed value of `spin0` currently is 4 (since one does not want the orbit-averaged evolution to have a lower PN order than the precession-averaged evolution), while `phase0` $\in \{0, 2, 3, 4, 5, 6\}$, so the default setting is 6. There is an option to get detailed information on evolution by passing `verbose=True`. In Table I, we give some examples of running this code to compute the spin tilts at infinity.

Appendix B: Derivation of bound on change in tilts for large eccentricities

Here we derive a bound on the change in the cosines of the tilts when evolving with orbit-averaged evolution from a large eccentricity to $e \nearrow 1$. Specifically, using the precession equations for the binary's spin vectors \mathbf{S}_A and orbital angular momentum unit vector $\hat{\mathbf{L}}$ used in the orbit-averaged code [Eqs. (7) in [30]], as well as $\cos \theta_1 = \hat{\mathbf{S}}_1 \cdot \hat{\mathbf{L}}$ and $M\omega = v^3$ (where circumflexes denote unit vectors), one finds that

$$\frac{d \cos \theta_1}{dt} = \frac{3v^6}{2(1-e^2)^{3/2}} \left(1 + \frac{m_2}{m_1} - \frac{Mm_2}{L} \chi_{\text{eff}} \right) \frac{m_2^2 \chi_2}{M^3} \times [\hat{\mathbf{S}}_1, \hat{\mathbf{S}}_2, \hat{\mathbf{L}}] \quad (\text{B1})$$

and the same expression for tilt 2 with the swap $1 \leftrightarrow 2$ in the indices. Here $\chi_{\text{eff}} = (\mathbf{S}_1/m_1 + \mathbf{S}_2/m_2) \cdot \hat{\mathbf{L}}/M$ is the effective spin and $[\hat{\mathbf{S}}_1, \hat{\mathbf{S}}_2, \hat{\mathbf{L}}] = \hat{\mathbf{S}}_1 \times \hat{\mathbf{S}}_2 \cdot \hat{\mathbf{L}}$ denotes the scalar triple product. We now use the leading expression

$$\frac{de^2}{dt} = -2 \frac{m_1 m_2}{M^3} \frac{v^8}{15(1-e^2)^{5/2}} (304 + 121e^2) \quad (\text{B2})$$

to convert the time derivative to an e^2 derivative, giving

$$\frac{d \cos \theta_1}{de^2} = -\frac{45(1-e^2)}{4v^2(304 + 121e^2)} \left(1 + \frac{m_2}{m_1} - \frac{Mm_2}{L} \chi_{\text{eff}} \right) \times \frac{m_2 \chi_2}{m_1} [\hat{\mathbf{S}}_1, \hat{\mathbf{S}}_2, \hat{\mathbf{L}}]. \quad (\text{B3})$$

We also have, from the Peters relation between semimajor axis and eccentricity [12],

$$\frac{1}{v^2} = \frac{a}{M} = \zeta \frac{e^{12/19}}{1-e^2} \left(1 + \frac{121}{304} e^2 \right)^{870/2299}, \quad (\text{B4})$$

where ζ is set by the value of v at some point in the evolution. Thus, we have

$$\frac{d \cos \theta_1}{de^2} = -\frac{45\zeta e^{12/19}}{1216} \left(1 + \frac{121}{304} e^2 \right)^{-1429/2299} \times \left(1 + \frac{m_2}{m_1} - \frac{Mm_2}{L} \chi_{\text{eff}} \right) \frac{m_2 \chi_2}{m_1} [\hat{\mathbf{S}}_1, \hat{\mathbf{S}}_2, \hat{\mathbf{L}}]. \quad (\text{B5})$$

We now specialize to $e^2 \in [e_{\text{trans}}^2, 1]$ and also take the maximum values of 1 for $|\chi_{\text{eff}}|$ and $|\hat{\mathbf{S}}_1, \hat{\mathbf{S}}_2, \hat{\mathbf{L}}|$ to simplify the upper bound, at the cost of some slight weakening. We also note that L increases with e from the Peters expression. We do not use $m_2/m_1 \leq 1$ since we do not have an upper bound on the m_1/m_2 one gets for the bound on tilt 2. We then obtain

$$\left| \frac{d \cos \theta_1}{de^2} \right| \leq \frac{45\zeta}{1216} \left(1 + \frac{121}{304} e_{\text{trans}}^2 \right)^{-1429/2299} \times \left(1 + \frac{m_2}{m_1} + \frac{Mm_2}{L_{\text{trans}}} \right) \frac{m_2 \chi_2}{m_1}. \quad (\text{B6})$$

Moreover, we have

$$\zeta = \frac{1 - e_{\text{trans}}^2}{v_{\text{trans}}^2 e_{\text{trans}}^{12/19}} \left(1 + \frac{121}{304} e_{\text{trans}}^2 \right)^{-870/2299}, \quad (\text{B7})$$

so an upper bound on the change in $\cos \theta_1$ between $e^2 = e_{\text{trans}}^2$ and $e^2 = 1$ is given by

$$\begin{aligned} |\Delta \cos \theta_1| &= \left| \int_{e_{\text{trans}}^2}^1 \frac{d \cos \theta_1}{de^2} de^2 \right| \\ &\leq (1 - e_{\text{trans}}^2) \max_{e^2 \in [e_{\text{trans}}^2, 1]} \left| \frac{d \cos \theta_1}{de^2} \right| \\ &\leq \frac{45(1 - e_{\text{trans}}^2)^2}{1216 v_{\text{trans}}^2 e_{\text{trans}}^{12/19}} \left(1 + \frac{121}{304} e_{\text{trans}}^2 \right)^{-1} \\ &\quad \times \left(1 + \frac{m_2}{m_1} + \frac{Mm_2}{L_{\text{trans}}} \right) \frac{m_2 \chi_2}{m_1}. \end{aligned} \quad (\text{B8})$$

(The analogous expression for $|\Delta \cos \theta_2|$ is obtained by taking $1 \leftrightarrow 2$ in the indices.) This is not the sharpest upper bound possible, but suffices for our purposes. Of course, we have used the leading-order Peters expression for the evolution of a with e as well as for de^2/dt , while the orbit-averaged evolution includes higher-PN corrections. However, for the applications we consider in Sec. V, these corrections are not large. In particular, noting that \bar{x} decreases with e from the Peters expression, the 1PN corrections to $d\omega/dt$ and de^2/dt that would give the 1PN corrections to the Peters expression are fractionally less than a 3% correction to the leading-order contributions (with the larger contribution for binary B, with its higher eccentricity). Thus, they are not a large correction to the bound we derived. We leave deriving a strict bound on the corrections from higher-PN terms to future work.

-
- [1] J. Aasi *et al.* (LIGO Scientific Collaboration), *Classical Quantum Gravity* **32**, 074001 (2015), arXiv:1411.4547 [gr-qc].
- [2] F. Acernese *et al.* (Virgo Collaboration), *Classical Quantum Gravity* **32**, 024001 (2015), arXiv:1408.3978 [gr-qc].
- [3] R. Abbott *et al.* (LIGO Scientific Collaboration, Virgo Collaboration, and KAGRA Collaboration), *Phys. Rev. X* **13**, 041039 (2023), arXiv:2111.03606 [gr-qc].
- [4] T. Akutsu *et al.* (KAGRA), *Prog. Theor. Exp. Phys* **2021**, 05A101 (2021), arXiv:2005.05574 [physics.ins-det].
- [5] B. P. Abbott *et al.* (KAGRA Collaboration, LIGO Scientific Collaboration, and Virgo Collaboration), *Living Rev. Relativity* **23**, 3 (2020), arXiv:1304.0670 [gr-qc].
- [6] M. Punturo *et al.*, *Classical Quantum Gravity* **27**, 194002 (2010).
- [7] M. Evans *et al.*, arXiv:2109.09882 [astro-ph.IM] (2021).
- [8] M. Colpi *et al.* (LISA Collaboration), arXiv:2402.07571 [astro-ph.CO] (2024).
- [9] M. Mapelli, in *Handbook of Gravitational Wave Astronomy*, edited by C. Bambi, S. Katsanevas, and K. D. Kokkotas (2021) p. 16.
- [10] R. Abbott *et al.* (LIGO Scientific Collaboration, Virgo Collaboration, and KAGRA Collaboration), *Phys. Rev. X* **13**, 011048 (2023), arXiv:2111.03634 [astro-ph.HE].
- [11] S. Stevenson, C. P. L. Berry, and I. Mandel, *Mon. Not. R. Astron. Soc.* **471**, 2801 (2017), arXiv:1703.06873 [astro-ph.HE].
- [12] P. C. Peters, *Phys. Rev.* **136**, B1224 (1964).
- [13] I. M. Romero-Shaw, P. D. Lasky, and E. Thrane, *Astrophys. J. Lett.* **921**, L31 (2021), arXiv:2108.01284 [astro-ph.HE].
- [14] V. Gayathri, J. Healy, J. Lange, B. O'Brien, M. Szczepanczyk, I. Bartos, M. Campanelli, S. Klimentko, C. O. Lousto, and R. O'Shaughnessy, *Nature Astron.* **6**, 344 (2022), arXiv:2009.05461 [astro-ph.HE].
- [15] I. M. Romero-Shaw, P. D. Lasky, E. Thrane, and J. Calderón Bustillo, *Astrophys. J. Lett.* **903**, L5 (2020), arXiv:2009.04771 [astro-ph.HE].
- [16] I. M. Romero-Shaw, P. D. Lasky, and E. Thrane, *Astrophys. J.* **940**, 171 (2022), arXiv:2206.14695 [astro-ph.HE].
- [17] N. Gupte *et al.*, arXiv:2404.14286 [gr-qc] (2024).
- [18] M. d. L. Planas, A. Ramos-Buades, C. García-Quirós, H. Estellés, S. Husa, and M. Haney, arXiv:2504.15833 [gr-qc] (2025).
- [19] G. Fumagalli, I. Romero-Shaw, D. Gerosa, V. De Renzi, K. Kritos, and A. Olejak, *Phys. Rev. D* **110**, 063012 (2024), arXiv:2405.14945 [astro-ph.HE].
- [20] N. K. Johnson-McDaniel, S. Kulkarni, and A. Gupta, *Phys. Rev. D* **106**, 023001 (2022), arXiv:2107.11902 [astro-ph.HE].
- [21] M. Mould and D. Gerosa, *Phys. Rev. D* **105**, 024076 (2022), arXiv:2110.05507 [astro-ph.HE].
- [22] A. M. Knee, J. McIver, and M. Cabero, *Astrophys. J.* **928**, 21 (2022), arXiv:2109.14571 [gr-qc].
- [23] S. Kulkarni, N. K. Johnson-McDaniel, K. S. Phukon, N. V. Krishnendu, and A. Gupta, *Phys. Rev. D* **109**, 043002 (2024), arXiv:2308.05098 [astro-ph.HE].
- [24] A. Klein *et al.*, arXiv:2204.03423 [astro-ph.HE] (2022).
- [25] G. Pratten, P. Schmidt, H. Middleton, and A. Vecchio, *Phys. Rev. D* **108**, 124045 (2023), arXiv:2307.13026 [gr-qc].
- [26] G. Fumagalli and D. Gerosa, *Phys. Rev. D* **108**, 124055 (2023), arXiv:2310.16893 [gr-qc].
- [27] K. Kritos, V. Stokov, V. Baibhav, and E. Berti, *Phys. Rev. D* **110**, 043023 (2024), arXiv:2210.10055 [astro-ph.HE].
- [28] D. Gerosa, G. Fumagalli, M. Mould, G. Cavallotto, D. P. Monroy, D. Gangardt, and V. De Renzi, *Phys. Rev. D* **108**, 024042 (2023), arXiv:2304.04801 [gr-qc].
- [29] LIGO-Virgo-KAGRA Algorithm Library - LALSuite, free software (GPL) (2025).
- [30] K. S. Phukon, N. K. Johnson-McDaniel, A. Singh, and A. Gupta, arXiv:2504.20543 [gr-qc] (2025).
- [31] `eccentric_bbh_evolution_lalsuite` git repository, https://gitlab.com/Amiteshh/eccentric_bbh_evolution_lalsuite/.
- [32] T. Damour and N. Deruelle, *Ann. Inst. Henri Poincaré Phys. Théor.* **43**, 107 (1985).
- [33] R.-M. Memmesheimer, A. Gopakumar, and G. Schäfer, *Phys. Rev. D* **70**, 104011 (2004), arXiv:gr-qc/0407049.
- [34] K. G. Arun, L. Blanchet, B. R. Iyer, and S. Sinha, *Phys. Rev. D* **80**, 124018 (2009), arXiv:0908.3854 [gr-qc].
- [35] N. Loutrel and N. Yunes, *Classical Quantum Gravity* **34**, 044003 (2017), arXiv:1607.05409 [gr-qc].
- [36] A. Klein and P. Jetzer, *Phys. Rev. D* **81**, 124001 (2010), arXiv:1005.2046 [gr-qc].
- [37] A. Klein, Y. Boetzel, A. Gopakumar, P. Jetzer, and L. de Vittori, *Phys. Rev. D* **98**, 104043 (2018), arXiv:1801.08542 [gr-qc].
- [38] É. Racine, *Phys. Rev. D* **78**, 044021 (2008), arXiv:0803.1820 [gr-qc].
- [39] M. Kesden, D. Gerosa, R. O'Shaughnessy, E. Berti, and U. Sperhake, *Phys. Rev. Lett.* **114**, 081103 (2015), arXiv:1411.0674 [gr-qc].
- [40] D. Gerosa, M. Kesden, U. Sperhake, E. Berti, and R. O'Shaughnessy, *Phys. Rev. D* **92**, 064016 (2015), arXiv:1506.03492 [gr-qc].
- [41] D. Gerosa, U. Sperhake, and J. Vošmera, *Classical Quantum Gravity* **34**, 064004 (2017), arXiv:1612.05263 [gr-qc].
- [42] H. Yu, S. Ma, M. Giesler, and Y. Chen, *Phys. Rev. D* **102**, 123009 (2020), arXiv:2007.12978 [gr-qc].
- [43] L. Blanchet, G. Faye, Q. Henry, F. Larrouturou, and D. Trestini, *Phys. Rev. Lett.* **131**, 121402 (2023), arXiv:2304.11185 [gr-qc].
- [44] X. Liu, Z. Cao, and Z.-H. Zhu, *Classical Quantum Gravity* **41**, 195019 (2024), arXiv:2310.04552 [gr-qc].
- [45] R. Gamba, D. Chiamello, and S. Neogi, *Phys. Rev. D* **110**, 024031 (2024), arXiv:2404.15408 [gr-qc].
- [46] B. Ireland, O. Birnholtz, H. Nakano, E. West, and M. Campanelli, *Phys. Rev. D* **100**, 024015 (2019), arXiv:1904.03443 [gr-qc].
- [47] N. Loutrel, S. Liebersbach, N. Yunes, and N. Cornish, *Classical Quantum Gravity* **36**, 025004 (2019), arXiv:1810.03521 [gr-qc].
- [48] G. Fumagalli, N. Loutrel, D. Gerosa, and M. Boschini, arXiv:2502.06952 [gr-qc] (2025).
- [49] R. Samanta, S. Tanay, and L. C. Stein, *Phys. Rev. D* **108**, 124039 (2023), arXiv:2210.01605 [gr-qc].
- [50] J. D. Hunter, *Comput. Sci. Eng.* **9**, 90 (2007).
- [51] C. R. Harris *et al.*, *Nature (London)* **585**, 357 (2020), arXiv:2006.10256 [cs.MS].
- [52] W. McKinney, in *Proceedings of the 9th Python in Science Conference*, edited by S. van der Walt and J. Millman (2010) pp. 51 – 56.
- [53] P. Virtanen *et al.*, *Nat. Methods* **17**, 261 (2020), arXiv:1907.10121 [cs.MS].